# *Precipitation in Kathmandu Valley: A Spatial-Temporal study*

Abstract

Over the past decade, advancements in atmospheric research have significantly improved the analysis of precipitation monitoring, understanding climate trends and variability, and identifying climatic anomalies associated with dry and wet periods. A key objective of this research is to enhance the understanding of precipitation patterns in the Kathmandu Valley, particularly in relation to the placement of gauges for long-range predictions and subsequent forecasting challenges. This study focuses on the evolving patterns of precipitation across the three districts within the Kathmandu Valley, the most developed and densely populated area in Nepal, encircled by four mountain ranges. We employ interpolation methods in ArcGIS Pro to identify, estimate, and forecast precipitation trends, and use the Mann-Kendall test to reveal statistically significant trends and provide insights into broader climatic processes. The research analyzes trends in both seasonal and annual precipitation and temperature across four time periods—pre-monsoon, monsoon, post-monsoon, and winter—using the Mann-Kendall test. The analysis reveals a decreasing trend in monthly rainfall from 2003 to 2017 at the majority of stations (14 stations out of 19), with areas along the valley slopes receiving significantly more precipitation compared to the central valley. The results of this study contribute to a deeper understanding of climate change in the Kathmandu Valley.

Keywords: Mann Kendell, Precipitation Trend, Climate change

## Introduction:

Climate change presents a significant and complex challenge for Nepal, particularly as a mountainous country where its effects are deeply felt across various aspects of life (Karki et al., 2009). The key climate variables—temperature and precipitation—play crucial roles in shaping the environment, impacting everything from human health to ecosystems, and affecting the survival of plants and animals. As global climate patterns shift, these changes are becoming more pronounced in Nepal, where communities that rely heavily on natural resources are increasingly vulnerable, yet often unaware of the full extent of the risks posed by climate change (Maharjan et al., 2011). Over the past 30 years, the Kathmandu Valley has experienced a steady temperature rise, a local manifestation of the broader, global phenomenon of climate change (Marahatta et al., 2009; Shrestha et al., 1999). This warming trend mirrors global climate shifts, underscoring the urgent need for awareness and adaptation strategies in this region.

Meteorological studies of the Kathmandu Valley reveal a noticeable decrease in the number of days with temperatures below 0°C, alongside an increase in the frequency of hot days, with temperatures climbing by 0.03°C annually. This pattern indicates that warmer days are becoming increasingly scorching, while cold days are experiencing more extreme cold (Shrestha et al., 2014).

Nationally, Nepal has seen a consistent rise in average temperatures, increasing at a rate of 0.05°C per year (DHM, 2008). In the Kathmandu Valley specifically, the maximum and minimum temperatures increased by 0.05°C and 0.04°C per year, respectively (Shrestha et al., 2014). These temperature changes are not just isolated events; they are part of a broader regional trend. For instance, Maskey et al. (2011) have documented a warming trend across the Himalayas, which is affecting the delicate balance of glaciers and snowpack. This disruption in the cryosphere is leading to changes in the availability of water resources, particularly during critical periods like spring and autumn. The implications of these shifts are profound, as they threaten the water supply, agriculture, and overall livelihoods of communities dependent on the seasonal meltwater from glaciers. This underscores the growing urgency for adaptive strategies to address the evolving climate dynamics in this region.

This study aims to analyze climate trends by employing the most current climatic data and advanced analytical methods. Earlier detailed analyses of historical climate trends were conducted by Practical Action Nepal (PAN) in 2009, using data spanning from 1976 to 2005, and by the Department of Hydrology and Meteorology (DHM) in 2015, with data from 1971 to 2012. Prior to these investigations, research often had a narrower focus, typically addressing only one climate variable—such as maximum temperature, precipitation, or extreme weather events—or examining trends at either a national average level or individual weather stations. Many earlier studies did not integrate multiple variables or regional data comprehensively, limiting their ability to capture the broader climate dynamics and changes over time.

Study Area:

The Kathmandu Valley, located centrally in Nepal, spans from 27°42' N to 85°18' E and covers approximately 220 square miles (570 km²). It is home to the capital city, Kathmandu, and is surrounded by the majestic Himalayas to the north and the Mahabharat Range to the south. The valley comprises several districts, including Kathmandu, Bhaktapur, and Lalitpur. Elevation within the Kathmandu Valley varies significantly, ranging from 1,200 meters to 2,750 meters above sea level. This elevation gradient contributes to a diverse range of climatic conditions across the valley, influenced by the surrounding mountainous terrain. The interplay of these geographical features creates a complex and varied climate, impacting local weather patterns and environmental conditions throughout the region

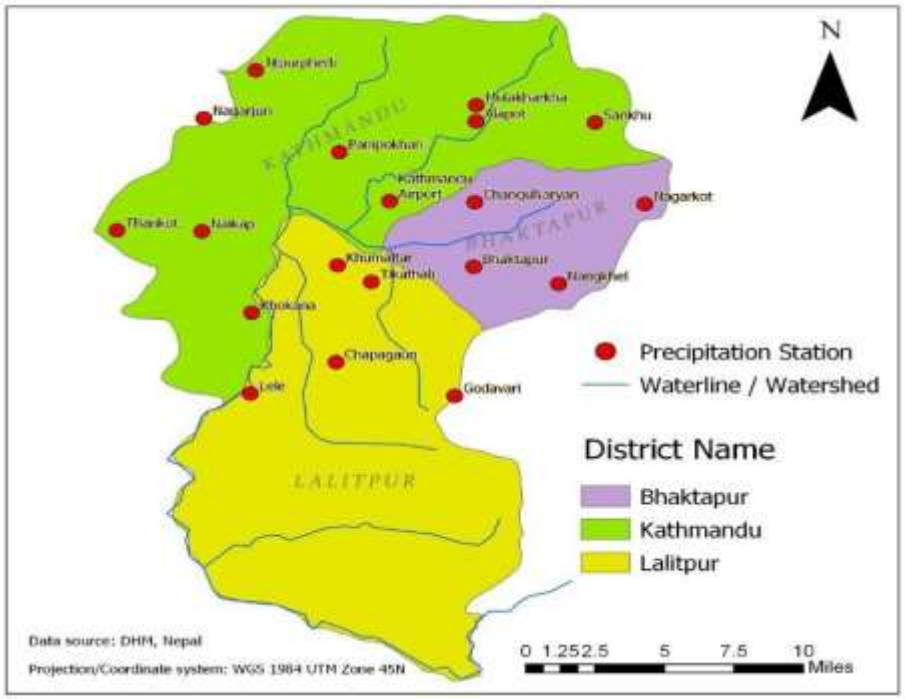


Map: Study map

Data:

For this study, we employed meteorological data from the Department of Hydrology and Meteorology (DHM), a government agency operating under the Ministry of Energy, Water Resources, and Irrigation. The DHM is a member of the World Meteorological Organization (WMO) and adheres to international standards for data collection and open access, facilitating research through data exchange protocols established by the WMO. We selected 19 weather stations with data covering the period from 2003 to 2018. These stations are spread across a range of elevations, from 1,212 meters at Khokhana to 2,163 meters at Nagarkot. They are strategically located across the Kathmandu Valley, extending from east to west between Nagarkot and Thankot, and north to south from Lele to Mulakharkha. This broad geographical coverage allows for a thorough analysis of precipitation patterns and trends throughout the valley..

*Table 1: Name of each station with their elevation, and, seasonal and annual rainfall in meters and millimeters respectively.*

| Stat._ID | Station | Lat | Lon | Elev(M | Pre_Mon. | Monsoon | Post_Mon. | Winter | Annual |
|---|---|---|---|---|---|---|---|---|---|
| 1015 | Thankot | 27.68 | 85.2 | 1630 | 233.7 | 1131.5 | 43.5 | 44.5 | 1461 |
| 1022 | Godavari | 27.58 | 85.4 | 1400 | 220.3 | 1226.5 | 51.1 | 39.4 | 1544 |
| 1029 | Khumaltar | 27.66 | 85.33 | 1350 | 207.1 | 853.1 | 42.4 | 33.6 | 1141.9 |

| | | | | | | | | | |
|---|---|---|---|---|---|---|---|---|---|
| 1030 | Kathmandu Airport | 27.7 | 85.36 | 1337 | 236.8 | 1148.7 | 58.6 | 35.8 | 1485.3 |
| 1035 | Sankhu | 27.75 | 85.48 | 1449 | 256.1 | 1327.7 | 49.3 | 37.5 | 1678.2 |
| 1039 | Panipokhari | 27.73 | 85.33 | 1335 | 201 | 1197.1 | 50.6 | 32.3 | 1484.9 |
| 1043 | Nagarkot | 27.7 | 85.51 | 2163 | 250.8 | 1389.7 | 60.9 | 29.4 | 1740.7 |
| 1052 | Bhaktapur | 27.66 | 85.41 | 1330 | 227.4 | 1000.2 | 55.1 | 30 | 1319.4 |
| 1059 | ChanguNaryan | 27.7 | 85.41 | 1543 | 257.4 | 1273.4 | 72.7 | 33.7 | 1655.6 |
| 1060 | Chapagaun | 27.6 | 85.33 | 1448 | 170.7 | 944.4 | 38.5 | 31.9 | 1192.7 |
| 1073 | Khokana | 27.63 | 85.28 | 1212 | 216.4 | 900.8 | 44 | 40.8 | 1209.8 |
| 1074 | Mulakharkha | 27.76 | 85.41 | 1490 | 279.1 | 1556.4 | 57.1 | 59.2 | 1960.3 |
| 1075 | Lele | 27.58 | 85.28 | 1590 | 212 | 1236.4 | 63.7 | 43.6 | 1561.9 |
| 1076 | Naikap | 27.68 | 85.25 | 1520 | 160 | 953.6 | 34.2 | 27.8 | 1180.3 |
| 1077 | Alapot | 27.75 | 85.41 | 1360 | 250.1 | 1508.2 | 55.8 | 31.2 | 1849.2 |
| 1079 | Nagarjun | 27.75 | 85.25 | 1690 | 211.1 | 1357.9 | 59.4 | 39.3 | 1675 |
| 1080 | Tikathali | 27.65 | 85.35 | 1341 | 186.8 | 885.2 | 55.9 | 31 | 1165.9 |
| 1081 | Jitpurphedi | 27.78 | 85.28 | 1320 | 233.7 | 1420.4 | 57.9 | 38.6 | 1756.5 |
| 1082 | Nangkhel | 27.65 | 85.46 | 1428 | 200.8 | 1023.4 | 47.3 | 32.3 | 1310.3 |

*Materials and method:*

*1) Modified Inversed Distance Weighting ($IDW_m$)*

The data provided by the Department of Hydrology and Meteorology (DHM) had a minor gap of approximately 2%, which is insignificant for the analysis. To handle the missing values, we employed a modified inverse distance weighting (IDW) technique, specifically designed to address the substantial altitude differences between stations. We utilized an updated version of the method introduced by Chang et al. (2005), which ensures that the sum of the weights equals one. This method accounts for both Euclidean distances and elevation differences (Barrios et al., 2018).

$$y_{j(m)} = \sum_{i=1}^{n} (h_{mi}^{-a} . d_{mi}^{-k} . x_{j(i)}) / \sum_{i=1}^{n} (h_{mi}^{-a} . d_{mi}^{-k})$$

In this approach, $h_{mi}$ denotes the absolute elevation difference between the target station and its neighboring stations, while *a* is a power parameter that influences the weighting based on elevation. By adjusting the weights to prioritize neighboring stations with similar or close elevations to the target station, this method provides more accurate estimates. Barrios et al. (2018) found that setting the exponent *a* and *k* to 1 yields the most effective results for interpolating missing precipitation values.

*2) Mann Kendell Test:*

The Mann-Kendall Trend Test, or M-K test, is employed to identify monotonic trends—whether consistently increasing or decreasing—in time series data. It is a non-parametric test, meaning it

does not require the data to be normally distributed, and is effective for any distribution, as long as there is no serial correlation. The test is frequently used in meteorological studies to determine significant trends (Dhital et al., 2013; Karki, 2017; Latif et al., 2018) and is often preferred over

parametric tests due to its simplicity (Yue & Wang, 2004). Rather than focusing on the actual values, the Mann-Kendall test compares the relative magnitudes of the data points (Gilbert, 1987). Its robustness to abrupt changes and irregularities in the time series further underscores its importance (Jaagus, 2006; Tabari & Talaee, 2011).

$$s = \sum_{k=1}^{n-1} \sum_{j=k+1}^{n} \operatorname{sgn}(x_j - x_{K)}$$

In the above equation, n is the number of points, and $x_k$ and $x_j$ are the data value in the time series *k* and *j (j>k)*, respectively. A positive *S* value shows an upward trend; a negative value indicates the downward trend, whereas zero means that there is no trend. Therefore, here, $sgn(x_j - x_k)$ is the sign function as described as follow:

$$\operatorname{sgn}(x) = \begin{Bmatrix} +1.....if.... (x_j - x_k) > 0 \\ 0.....if ..... (x_j - x_k) = 0 \\ -1.....if .....(x_j - x_k) < 0 \end{Bmatrix}$$

The significance of the trend is evaluated by calculating the statistics *sgn(x)*. The scattering (variance) $\sigma^2$ is estimated by,

$$Var(s)\{\sigma^2\} = \{n(n-1)(2n+5) - \sum_{j=1}^{p} t_j (t_j - 1)(2t_j + 5)\}/18$$

Where p is the number of the tied groups in the data set, n is the number of series, and $t_j$ is the number of data points in the jth tied group. In a case where n>10, the standard normal test statistics Z is computed using the above variance equation as follow,

$$z_{mk} = \begin{Bmatrix} \dfrac{s-1}{\sqrt{Var(s)}} .....if .....S > 0 \\ 0.....if .....S = 0 \\ \dfrac{s+1}{\sqrt{Var(s)}} .....if .....S < 0 \end{Bmatrix}$$

The trend is analyzed at a specific α significance level. Therefore, if the probability under the null hypothesis ($H_o$) of observing value higher than the test statistics $Z_{mk}$ for a chosen significance level α, this indicates a statistically significant trend. The null hypothesis $H_o$ is considered true if there is no trend, and that uses the standard normal table to decide whether to reject $H_o$. to test for either an upward or downward trend ( a two-tailed test) at α level of significance, $H_o$ is negative if the absolute value of $Z_{mk} > Z_{1-\alpha/2}$ at the α-level of significance.

*3) Sen's slope estimator*

The magnitude of the trend slopes by Sen's method is used to see the change over time is calculated as follow:

$$Q_i = \frac{x_j - x_k}{j - k} if \ldots j > k$$

Where $x_j$ and $x_k$ represent the annual values throughout the years j and k, respectively. The Sen's estimator of slopes provides the median of these N values of slopes (Q). The median of the N slopes estimates was obtained in by simple averaging. N values of $Q_i$ were ranked from smallest to largest, and the Sen's estimator was computed as follows:

Sen's estimator:

$$Q_i = \begin{cases} Q_{\left\lceil \frac{N+1}{2} \right\rceil} \ldots if \text{ N was Odd} \\ \frac{1}{2}\left(Q_{\frac{N}{2}} + Q_{[(N+2)/2]}\right) \ldots if \text{ N was Even} \end{cases}$$

Finally, Sen's estimator was tested using a two-sided test at the 100(1-α) % confidence interval, and the true slope may be obtained by the non-parametric test (*Latif et al. 2016*).

4) *Empirical Bayesian Kriging (EBk*):

Empirical Bayesian kriging (EBK) is a geo-statistical interpolation method that automates the most difficult aspects of building a valid kriging model. Other kriging methods in Geostatistical analysts require you to adjust parameters to receive accurate results manually, but EBK automatically calculates these parameters through a process of sub setting and simulations (Krivoruchko K. 2012). This method interpolated the difficult rainfall aspect of spatially a valid kriging model(Baker et al., 2015). Empirical Bayesian kriging also differs from other kriging methods by accounting for the error introduced by estimating the underlying semi-variogram. Other kriging methods calculate the semi-variogram from known data locations and use this single semi-variogram to make predictions at unknown locations; however, this process assumes that the estimated semi-variogram is the true semi-variogram for the interpolation region. The Empirical Bayesian Kriging is calculated as follows (Goovaerts, 2005):

$$\gamma_{ebk} u_\alpha = \lambda u_\alpha Z u_\alpha + \left[1 - \lambda u_\alpha\right] m$$

Where m is the population-weighted sample mean, λ ($u_\alpha$) is the weight assigned to the rate observed at locations $u_{\alpha.}$

The semi-variograms and covariance functions quantify the assumptions that rainfall series nearby tend to be more similar than rainfall series in various stations that are further apart. The semi-variograms, covariance, and correlation functions are theoretical quantities that estimate them from rainfall using tool is called the empirical semi-variograms, empirical covariance, and correlation functions. These functions are calculated as follows (Bohling, 2005; I. Gundogu, 2015; Oliver and Webster, 2015; Scheuerer & Hamil, 2015).

Correlation function:

$$R \times h = \frac{C \times h}{\sqrt{\sigma_0 \times \sigma_{+h}}}$$

Covariance Function:

$$C \times h = \frac{1}{nh} \sum_{\alpha=1}^{n(h)} Zu_\alpha \times Zu_\alpha + h - m_0 \times m_{+h}$$

Semi variance functions:

$$\gamma h = \frac{1}{nh} \sum_{\alpha=1}^{n(h)} \left[ Zu_\alpha + h - zu_\alpha \right]^2$$

Where $m_o$ and m are the means of the range values:

$$m_0 = \frac{1}{nh} \sum_{\alpha=1}^{n(h)} Zu_\alpha \text{ , and, } m_{+h} = \frac{1}{nh} \sum_{\alpha=1}^{n(h)} Zu_\alpha + h$$

Similarly, $\sigma_o$ and $\sigma_{+h}$ are the corresponding standard deviations:

$$\sigma_{+h} = \frac{1}{nh} \sum_{\alpha=1}^{n(h)} \left[ Zu_\alpha + h - m_{+h} \right]^2 \text{ , and, } \sigma_o = \frac{1}{nh} \sum_{\alpha=1}^{n(h)} \left[ Zu_\alpha - m_o \right]^2$$

Where u is a vector of spatial coordinates, z(u) is variable under consideration as a function of spatial location, h is a lag vector representing the separation between two spatial locations, and z(u+h) is a lagged version of the variable.

Result and discussion:

Here we analyzed precipitation data from 19 stations over the period 2003 to 2018, employing interpolation techniques within ArcGIS Pro. The identification, estimation, and forecasting of precipitation trends are crucial for advancing our understanding of broader climatic processes. Such trends provide essential insights into the statistical and physical dynamics of the climate system. To robustly detect these trends, we utilized the Mann-Kendall test, a well-established non-parametric method, across each data grid. This methodological approach ensures that the detected trends are statistically significant and relevant for further climatological investigations.

*Spatial Pattern of Precipitation*

Nepal's seasonal climate is divided into four distinct periods: pre-monsoon, monsoon, post-monsoon, and winter (Dhital et al., 2013; DHM, 2002). The pre-monsoon season refers to rainfall during March, April, and May; the monsoon season encompasses June, July, August, and September; the post-monsoon season includes October and November; and the winter season covers December, January, and February.

In this study, we utilized two geostatistical tools to examine the spatial patterns of precipitation. The empirical kriging tool was employed to model the rainfall distribution by constructing a semi-variogram, which provided insights into the spatial structure and allowed for the prediction of rainfall at unobserved locations. Additionally, the Inverse Distance Weighting (IDW) spatial analyst tool was applied to interpolate missing rainfall data across the 19 stations, facilitating a more complete and accurate representation of the spatial rainfall patterns in the region.

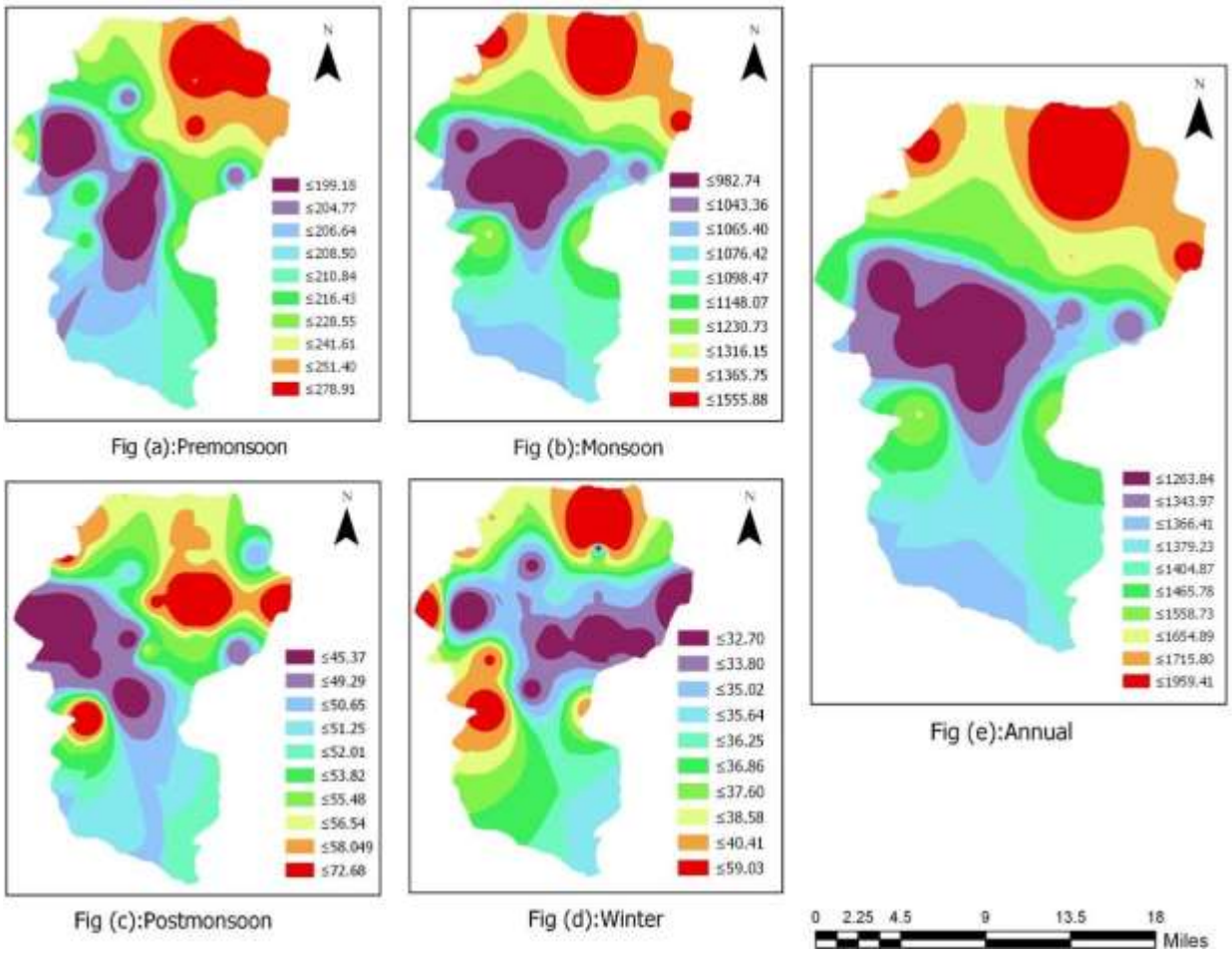


*Figure 1:Sesaonal and annual Interpolation of rainfall using IDW tool*

The interpolation of seasonal and mean annual precipitation data over the past 16 years, utilizing the Inverse Distance Weighting (IDW) methodology, is illustrated in Figure 1. The dataset, furnished by the Department of Hydrology and Meteorology, Nepal, originally contained 45 missing data points out of a total of 3,420 grid points. The IDW technique adeptly interpolated these deficiencies, facilitating a thorough spatial analysis.

The analysis reveals that the Kathmandu Valley acquires approximately 80% of its annual precipitation during the monsoon season, with the most substantial rainfall concentrations localized in the northern, northeastern, and northwestern sectors of the valley. During the pre-monsoon period, significant precipitation is also concentrated in the northeastern and northern

regions. These precipitation patterns are predominantly governed by easterly winds emanating from the Bay of Bengal, which convey considerable moisture to the eastern flank of the valley throughout all seasons except winter. Consequently, the eastern regions of the valley consistently receive more precipitation than the western regions, reflecting broader hydrometeorological trends in Nepal, where eastern regions generally experience more abundant rainfall than their western counterparts (Baidya, Shrestha, & Sheikh, 2008).

The Kathmandu Valley receives an average of approximately 1,500 mm of precipitation annually, with 1,200 mm occurring during the monsoon season alone. Furthermore, the data indicate that rainfall intensity is greater on the mountain slopes relative to the valley floor, a finding corroborated by Karki (2017).

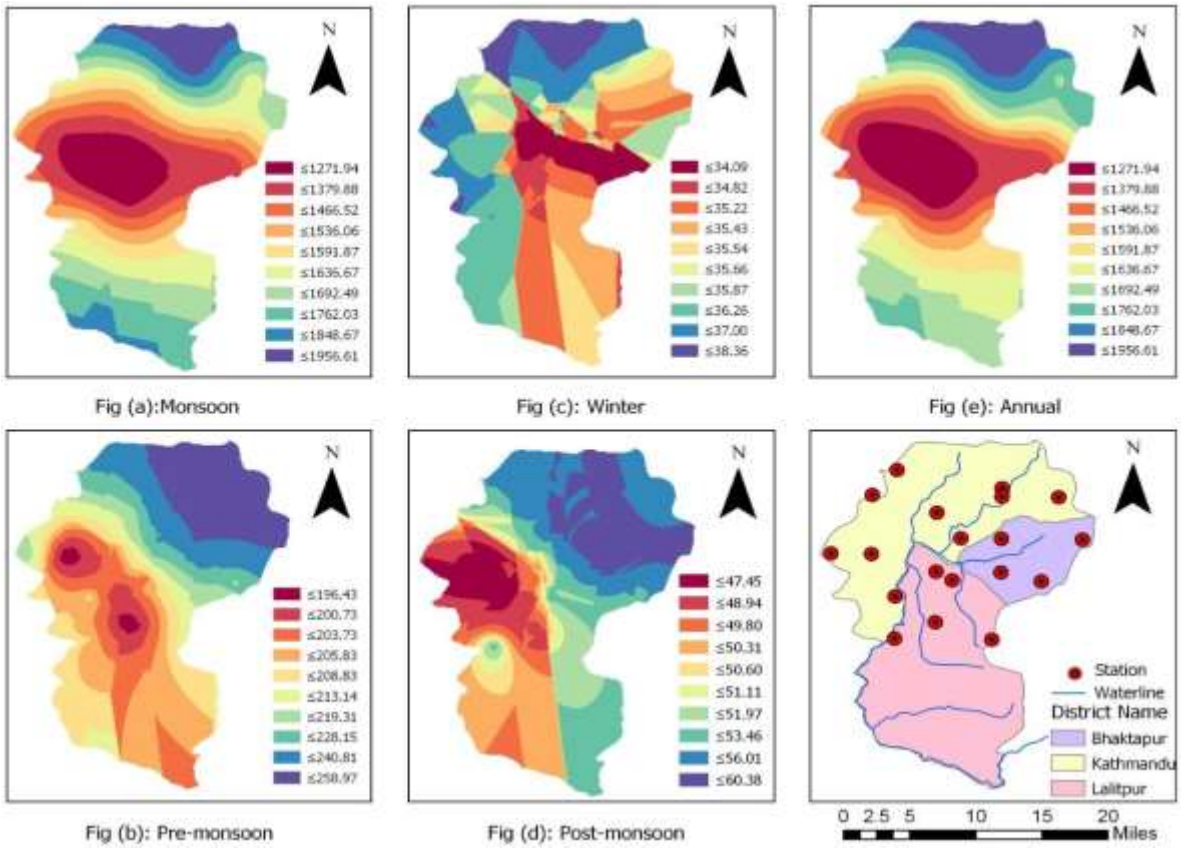


*Figure 2: Seasonal and annual Interpolation of rainfall using the Empirical Kriging Method*

Conversely, post-monsoon precipitation predominantly affects the central and western portions of the valley, while winter precipitation, driven by western disturbances originating from the Mediterranean Sea, is more pronounced in the western regions of the valley. In sum, the findings presented in Figure 1 underscore that monsoon rainfall is the principal determinant of annual precipitation trends in the Kathmandu Valley. Any fluctuations in monsoon patterns are likely to precipitate significant alterations in the overall annual precipitation distribution.

Figure 2 presents rainfall distribution across the Kathmandu Valley, derived through Empirical Bayesian Kriging Method. The analysis reveals that the northern sector of the valley remains perennially humid, receiving substantial precipitation throughout the year. During the monsoon

season, the northern and southern regions exhibit heightened rainfall intensity, whereas the central valley experiences comparatively diminished precipitation. Conversely, the winter rainfall pattern indicates a predilection for wetter conditions in the northwestern, southwestern, and western areas of the valley, in contrast to the relatively drier eastern regions. In the pre-monsoon period, the northern mountainous terrain of the valley is subject to significant rainfall accumulation. Similarly, during the post-monsoon season, the northeastern, eastern, and southeastern regions receive a notable amount of precipitation, surpassing that observed in the western sector. Overall, the annual rainfall distribution strongly correlates with the monsoonal precipitation pattern, underscoring the monsoon's pivotal influence on the valley's annual hydrometeorological dynamics.

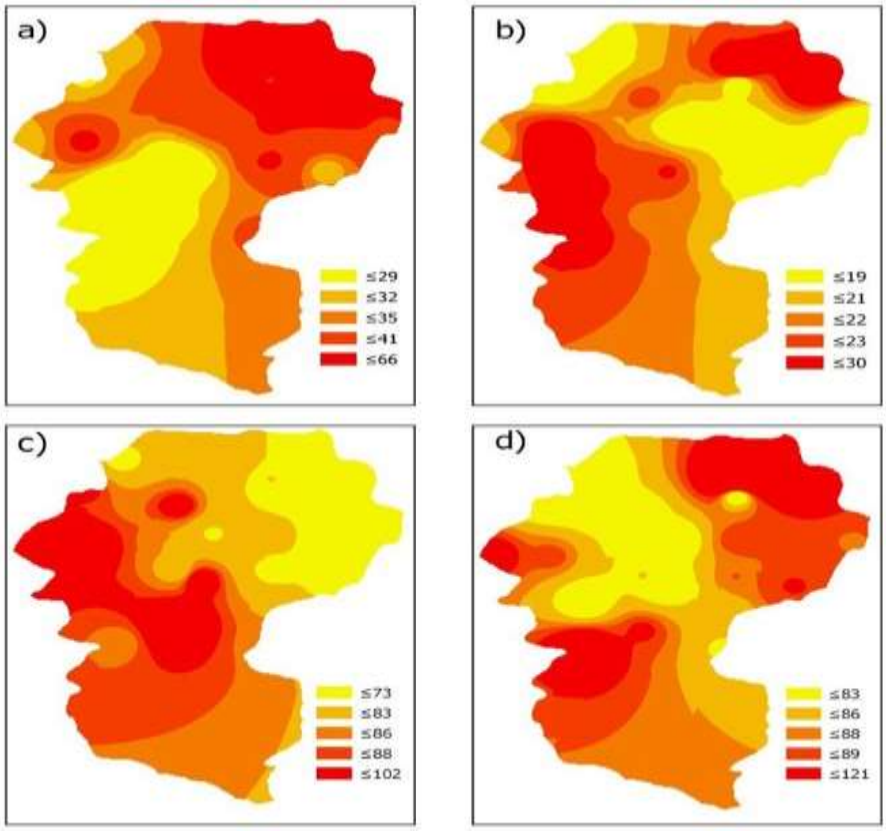


*Figure 3: Spatial Pattern of seasonal precipitation's CV's a) Pre-monsoon, b) Monsoon c) Post monsoon and d) Winter*

Figure 3 illustrates the Coefficient of Variation (CV) maps for precipitation, showcasing notable seasonal variations within the Kathmandu Valley. During the monsoon season, the valley is characterized by a CV of less than or equal to 30%, signifying consistently elevated and frequent precipitation across the entire region. This low variability underscores the overwhelming dominance of monsoonal rainfall during this period.

In stark contrast, the pre-monsoon season exhibits a pronounced increase in CV throughout the valley, reaching a peak of 66%. This heightened variability indicates that precipitation during this period is more erratic, contributing approximately 10% to the total annual rainfall. The pre-

monsoon season is typified by brief, intense rain events, often accompanied by thunderstorms and powerful easterly winds, which can precipitate severe weather phenomena and natural disasters across the valley.

The post-monsoon and winter seasons are characterized by significantly reduced precipitation, with correspondingly low mean rainfall. The post-monsoon CV reveals marked spatial variability, particularly within the western regions of the valley, where precipitation is markedly less consistent compared to the eastern regions. This variability likely results from the weakening atmospheric dynamics, wherein much of the moisture precipitates in the east before reaching the western areas. During the winter season, the CV is predominantly influenced by western disturbances, leading to sporadic and scattered rainfall across the valley. This season's variability reflects an unpredictable and irregular distribution of precipitation, further accentuating the impact of transient meteorological systems.

*Trend analysis of precipitation*

The spatial analysis of the Mann-Kendall (MK) trend test for seasonal rainfall is presented in Figure 4, while Figure 5 portrays the corresponding trends for annual precipitation. The analysis reveals that, aside from the southern stations (Lele and Chapagaun), central stations (Khumaltar, Kathmandu Airport, and Changunarayan), northern stations (Mulakharkha and Alapot), and the western station (Thankot), all other stations exhibit a discernible decreasing trend in pre-monsoon precipitation, as illustrated in Figure 4a. Nevertheless, it is important to note that none of these stations, with the exception of Naikap, display statistically significant trends in pre-monsoon rainfall. These observations are congruent with the findings of Dhital et al. (2013), Practical Action (2009), and Sada et al. (2013).

Among the 19 stations analyzed, five stations exhibit a positive trend in precipitation, while 74% display a decreasing trend. The stations with positive trends include Nagarjun (21), Jitpurphedi (16), Alapot (25), Mulakharkha (27), and Kathmandu Airport (15), with magnitudes of -2.05, 4.50, 15.13, 69, and 16.06, respectively, as calculated using Sen's slope Mann-Kendall test, as depicted in Figure 4b. Despite 26% of the stations showing an upward trend and the remainder showing a downward trend, none of these trends are statistically significant.

The spatial analysis of the Mann-Kendall test for the post-monsoon season reveals that 12 stations exhibit a downward trend, six stations show an upward trend, and one station displays no change, as illustrated in Figure 4c. Stations with a positive trend, though not statistically significant, include the western stations {Thankot (23) and Nagarjun (13)}, the central station {Kathmandu Airport (5)}, the northern stations {Mulakharkha (33) and Alapot (1)}, and the eastern station {Nangkhel (11)}. Notably, Panipokari (0) is the only station in the Kathmandu Valley that shows no significant trend change in post-monsoon rainfall. Similar to the monsoon season, no station in the Kathmandu Valley exhibits a statistically significant trend. Typically, winter rainfall in Nepal is characterized by irregularity, attributed to sporadic showers moving from west to east. Our analysis reveals that all stations in the Kathmandu Valley exhibit a negative trend in winter precipitation, none of which are statistically significant, as depicted in Figure 4d. This observation aligns with the findings of Dhital et al. (2013), who reported that precipitation patterns during the period from 1980 to 2009 did not exhibit significant increases or decreases.

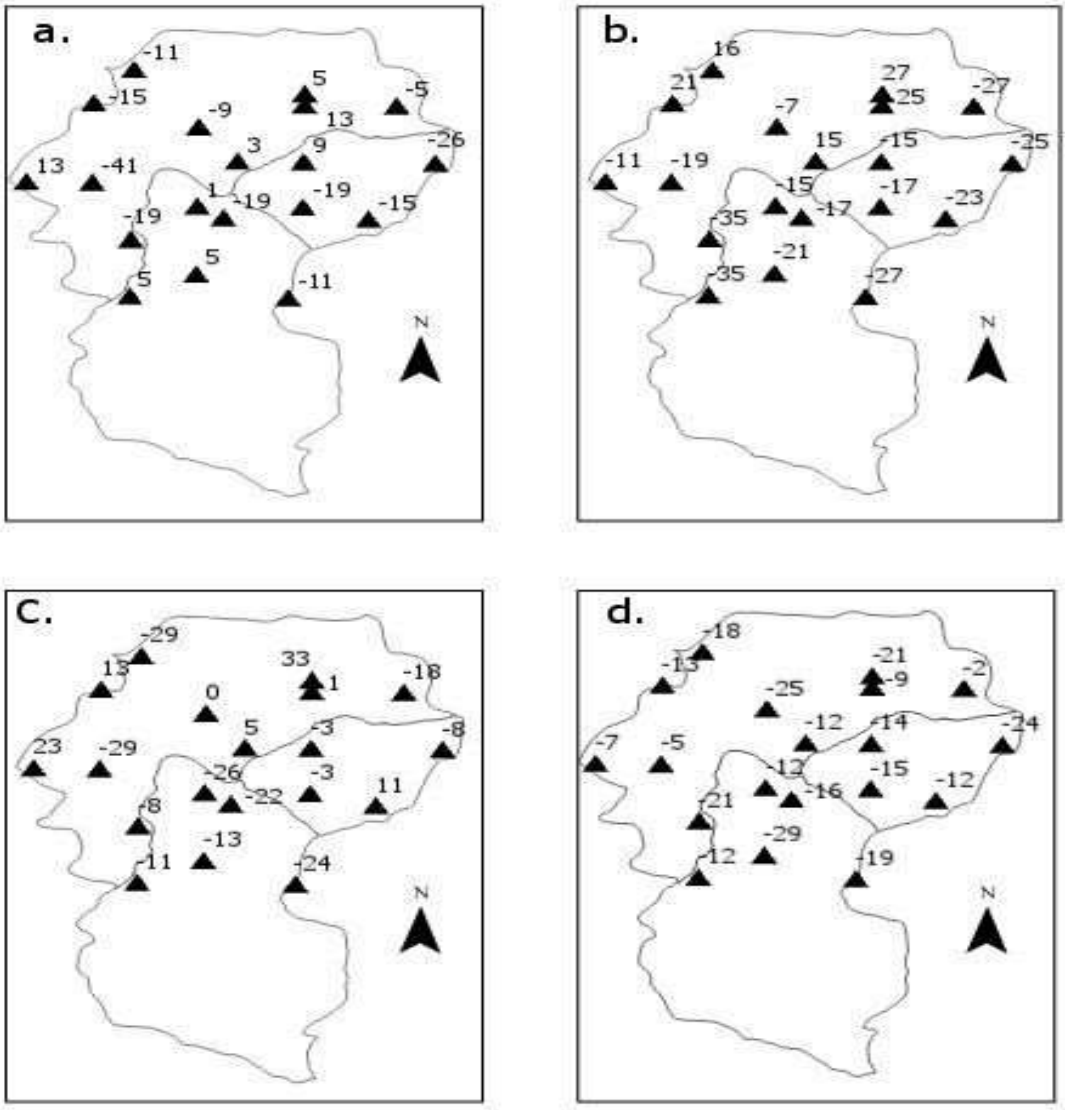


*Figure 4: Spatial Trend analysis of precipitation in a) Premonsoon b)Monsoon c)Postmonsoon d)Winter*

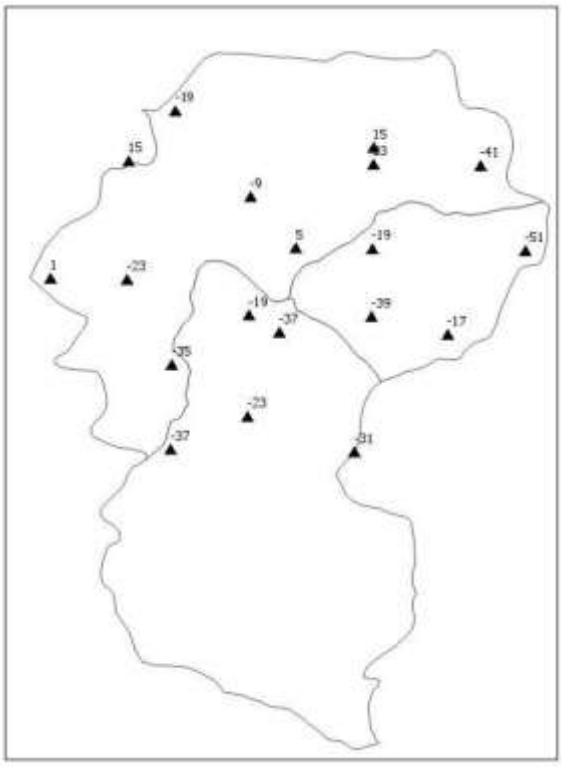


*Figure 5: Annual precipitation trend in Kathmandu Valley from 2003-2017*

Figure 5 elucidates the annual precipitation trends throughout the Kathmandu Valley, highlighting that only five stations exhibit a discernible upward trend. Notably, Mulakharkha and Alapot demonstrate increases in rainfall across both seasonal and annual analyses, with the exception of winter for the northern stations.

The omission of Jitpurphedi from the monsoon trend analysis and Thankot from the annual trend analysis accentuates the preeminence of monsoon rainfall in shaping the annual precipitation pattern, given that over 80% of the total annual precipitation is attributed to the monsoon season.

Although positive trends are discerned at stations such as Thankot, Nagarjun, Kathmandu Airport, Mulakharkha, and Alapot, these trends do not achieve statistical significance. Conversely, the downward trends observed at Nagarkot and Sankhu stations are statistically significant, signifying a marked decline in precipitation at these locations.

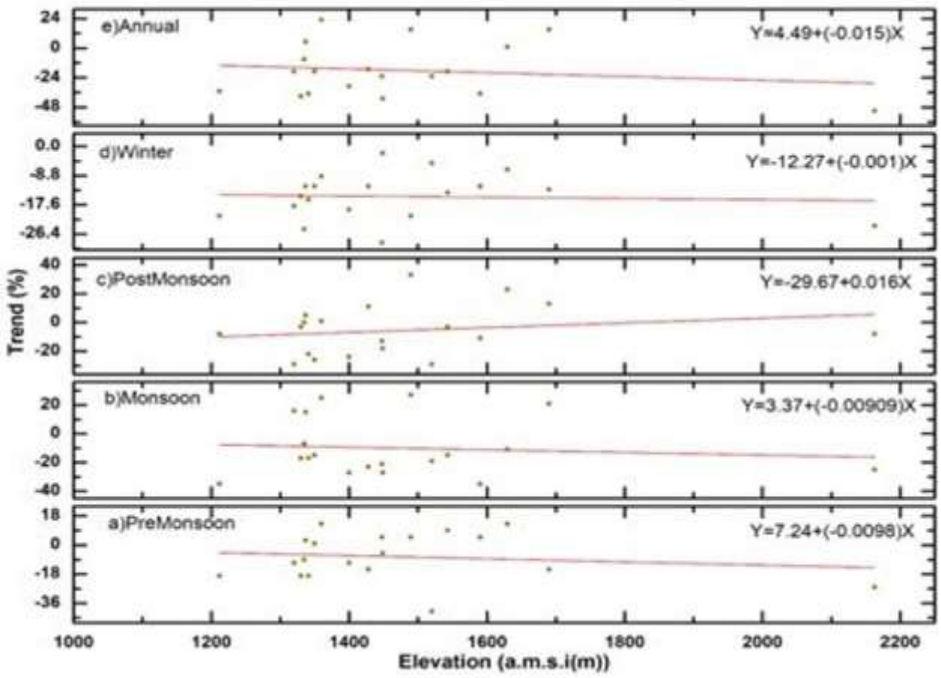


*Figure 6: Annual and seasonal Distribution of precipitation trends plotted against elevation*

Figure 6 presents the trend analysis of seasonal and annual rainfall relative to elevation, based on data from 19 meteorological stations within the Kathmandu Valley. The analysis indicates a predominant downward trend in rainfall across all seasons and annual totals at most of the stations. Specifically, with the exception of the post-monsoon season, all other seasonal rainfall trends from 2003 to 2017 display a negative trajectory.

Stations that show positive trends are primarily located at elevations ranging from 1,300 to 1,700 meters. The observed variability in rainfall trends within this elevation range can be attributed to the limited number of stations both above 1,700 meters and below 1,300 meters. This distribution gap likely contributes to the significant fluctuations observed in the trend analysis for these elevations

Conclusion:

This research examines the spatial and temporal patterns of annual and seasonal total rainfall in the Kathmandu Valley, utilizing precipitation data from 19 meteorological stations distributed throughout the region. The primary objective of this study was to evaluate the impact of climate change on precipitation trends and assess its implications for the valley's watershed.

Our analysis reveals a consistent decreasing trend in monthly rainfall across the majority of the stations from 2003 to 2017. Notably, areas along the valley slopes experience significantly higher precipitation compared to the central valley. The observed decline in monsoon rainfall is particularly concerning, given that this season contributes over 80% of the valley's total annual precipitation. This trend could have profound implications for local water resources and river discharge, as Kathmandu's water supply is heavily reliant on monsoonal rains.

Furthermore, reduced rainfall is likely to impact agricultural productivity in the lowland regions surrounding the Kathmandu Valley and could adversely affect hydropower generation. These findings highlight the urgent need for an in-depth analysis and immediate policy intervention to address the challenges posed by climate change and to ensure the sustainability of the valley’s vital water resources and agricultural systems.

Reference:


Baidya, S., Shrestha, M., & Sheikh, M. (2008). Trends in daily climatic extremes of temperature and precipitation in Nepal. *Journal of Hydrology and Meteorology*, *5*(1), 38-51.

Baker, B. H., Kröger, R., Brooks, J. P., Smith, R. K., & Czarnecki, J. M. P. (2015). Investigation of denitrifying microbial communities within an agricultural drainage system fitted with low-grade weirs. *Water Research, 87*, 193-201. https://doi.org/10.1016/j.watres.2015.09.028

Barrios, A., Trincado, G., & Garreaud, R. (2018). Alternative approaches for estimating missing climate data: Application to monthly precipitation records in South-Central Chile. *Forest Ecosystems, 5*(1), 28. https://doi.org/10.1186/s40663-018-0147-x

Chang, C. L., Lo, S. L., & Yu, S. L. (2006). The parameter optimization in the inverse distance method by genetic algorithm for estimating precipitation. *Environmental Monitoring and Assessment, 117*(1-3), 145–155. https://doi.org/10.1007/s10661-006-8498-0

Dhital, Y. P., Tang, Q., & Shi, J. (2013). Hydroclimatological changes in the Bagmati River Basin, Nepal. *Journal of Geographical Sciences, 23*(4), 612-626. https://doi.org/10.1007/s11442-013-1034-3

DHM (2002). Department of Hydrology and Meteorology, Babarmahal, Kathmandu, Nepal.

DHM (2008). Department of Hydrology and Meteorology, Babarmahal, Kathmandu, Nepal.

Gilbert, R. O. (1987). *Statistical methods for environmental pollution monitoring*. John Wiley & Sons.

Goovaerts, G. (2005). *Geostatistics for natural resources evaluation*. Oxford University Press.

Gundogdu, I. (2015). Usage of multivariate geostatistics in interpolation processes for meteorological precipitation maps. *Theoretical and Applied Climatology*, 1-6. https://doi.org/10.1007/s00704-015-1619-3

Hu, Y., Maskey, S., & Uhlenbrook, S. (2012). Trends in temperature and rainfall extremes in the Yellow River source region, China. *Climatic Change, 110*(1), 403-429. https://doi.org/10.1007/s10584-011-0056-2

Jaagus, J. (2006). Climatic changes in Estonia during the second half of the 20th century in relationship with changes in large-scale atmospheric circulation. *Theoretical and Applied Climatology, 83*(1–4), 77–88. https://doi.org/10.1007/s00704-005-0161-0

Karki, R. (2017). Rainfall variability over Kathmandu Valley: A study of daily rainfall pattern and its changes in Kathmandu Valley, Nepal during summer monsoon season.

Krivoruchko, K. (2012). *Bayesian hierarchical modeling for spatial data: Applications in environmental and ecological studies*. Springer.

Latif, Y., Yaoming, M., & Yaseen, M. (2018). Spatial analysis of precipitation time series over the Upper Indus Basin. *Theoretical and Applied Climatology, 131*(1–2), 761–775. https://doi.org/10.1007/s00704-016-2007-3

Maharjan, S., Sigdel, E., Sthapit, B., & Regmi, B. (2011). Tharu community's perception on climate changes and their adaptive initiations to withstand its impacts in Western Terai of Nepal. *International NGO Journal*, *6*(2), 35-42.

Marahatta, S., Dongol, B. S., & Gurung, G. B. (2009). Temporal and spatial variability of climate change over Nepal (1976-2005). *Practical Action Nepal*, Kathmandu.

Oliver, M. A., & Webster, R. (2015). *Basic steps in geostatistics: The variogram and kriging*. Springer.

Qing, Y., Zhu-Guo, M., & Liang, C. (2011). A preliminary analysis of the relationship between precipitation variation trends and altitude in China. *Atmospheric and Oceanic Science Letters, 4*(1), 41–46. https://doi.org/10.1080/16742834.2011.11446899

Sada, R., Shrestha, A., Karki, K., & Shukla, A. (2013). Groundwater extraction: Implications on local water security of peri-urban area of Kathmandu Valley. *Nepal Journal of Science and Technology*, *14*(1), 121-128. https://doi.org/10.3126/njst.v14i1.8932

Scheuerer, M., & Hamill, T. M. (2015). Variogram-based proper scoring rules for probabilistic forecasts of multivariate quantities. *Monthly Weather Review, 143*(4), 1321-1334.

Shrestha, A. B., Wake, C. P., Mayewski, P. A., & Dibb, J. E. (1999). Maximum temperature trends in the Himalaya and its vicinity: An analysis based on temperature records from Nepal for the period 1971–94. *Journal of Climate, 12*(9), 2775-2786.

Tabari, H., & Talaee, P. H. (2011). Temporal variability of precipitation over Iran: 1966-2005. *Journal of Hydrology, 396*(3–4), 313–320. https://doi.org/10.1016/j.jhydrol.2010.11.034

Viale, M., & Garreaud, R. (1955). *Journal of Geophysical Research*. Nature, 175(4449), 238. https://doi.org/10.1038/175238c0

Yue, S., & Wang, C. Y. (2004). The Mann-Kendall test modified by effective sample size to detect trend in serially correlated hydrological series. *Water Resources Management, 18*(3), 201–218. https://doi.org/10.1023/B:WARM.0000043140.61082.60